# Observation of the Volume Transition in Thermosensitive Core−Shell Latex Particles by Small-Angle X-ray Scattering

**N. Dingenouts, Ch. Norhausen, and M. Ballauff***

*Polymer-Institut, Universität Karlsruhe, Kaiserstrasse 12, 76128 Karlsruhe, Germany*

*Received June 23, 1998*

ABSTRACT: An investigation of the volume transition in colloidal core−shell particles composed of a temperature-independent polystyrene core and a shell of thermosensitive cross-linked polymer chains by small-angle X-ray scattering (SAXS) is presented. The PS cores of the particles have a diameter of 80 nm whereas the shell composed of cross-linked poly(*N*-isopropylacrylamide) has a thickness of 32 nm in the swollen state at 25 °C and of 18 nm after shrinking by a continuous volume transition. The SAXS intensities measured at high scattering angles could be described by a Lorentz-type function at both states. This indicates the presence of liquidlike local concentration fluctuations of the gel which are still present in the shrunken state. The correlation lengths $\xi$ measured in both states are of the order of a few nanometers (25 °C, $\xi = 3.2$ nm; 50 °C, $\xi = 2.1$ nm). The present analysis therefore shows that the core−shell microgels behave in a distinctively different manner than ordinary thermosensitive gels: The cross-linked chains in the shell are bound to a solid boundary independent of temperature. The spatial constraint by this boundary decreases the maximum degree of swelling but also prevents a full collapse of the network above the volume transition.

## Introduction

Gels composed of cross-linked poly(*N*-isopropylacrylamide) (PNIPA) chains may undergo a volume transition as a function of temperature in which the network shrinks in a continuous or discontinuous fashion.[1] If cross-linked PNIPA chains are affixed to the surface of polymer latex spheres, thermosensitive colloidal particles result. Such systems have been prepared recently by Makino et al.[2] and by Okubo et al.[3] and have attracted much interest because of their potential use for controlled drug delivery.[4] Colloidal particles composed of a solid polymer core and a temperature-sensitive cross-linked polymer shell, however, present interesting examples of micronetworks having a well-defined geometry. Thus, fixing the ends of the cross-linked PNIPA chains to a solid polystyrene (PS) core defines one boundary of the micronetwork which stays constant during the transition. In this respect such core−shell latex particles present cross-linked polymer brushes on defined spherical surfaces for which the solvent quality may be changed from good solvent conditions at room temperature to poor solvent conditions at a temperature above 34 °C.

In this paper we present a study of the volume transition of thermosensitive colloidal PS−PNIPA/core−shell particles composed of a PS core and a cross-linked PNIPA shell. The analysis of these particles which are dispersed in water has been done by small-angle X-ray scattering (SAXS). Previous investigations[5,6] have demonstrated that SAXS is highly suited to elucidate the radial structure of composite latex particles. In particular, SAXS allows one to study the structure of polymers and surfactants affixed to PS cores. This is due to the fact that PS has a low SAXS contrast toward water (6.4 $e^-/nm^3$; ref 5) whereas most polar polymers containing oxygen or nitrogen atoms exhibit a much higher contrast (PNIPA: 45.8 $e^-/nm^3$; see below). Hence, the measured SAXS intensity $I(q)$ ($q = (4\pi/\lambda)\sin(\theta/2)$; $\theta$, scattering angle; $\lambda$, wavelength) originates mainly from the shell.

The particles investigated here have been synthesized in two steps: First, PS particles containing a small amount of PNIPA are made by a conventional emulsion polymerization. These particles were used as the seeds in a second emulsion polymerization in which they were covered by a shell of cross-linked PNIPA chains. The radial structure of both the seed latex particles and the core−shell particles has been studied by SAXS. It is hence possible to characterize the shell in detail and to analyze the volume transition of the cross-linked PNIPA chains.

## Theory

The measured scattering intensity $I(q)$ of a suspension of noninteracting micronetwork particles contains in principle three independent contributions, the origin of which is depicted in Figure 1:

$$I(q) = I_{CS}(q) + I_{network}(q) + I_{PS}(q) \qquad (1)$$

Here, $I_{CS}(q)$ is the part of $I(q)$ due to the core−shell structure of the particles (i.e., the scattering intensity caused by composite particles having a homogeneous core and shell). The core and the shell are characterized by a different electron density shown schematically in Figure 1. The shell, however, does not consist of a solid material but of a polymeric network which exhibits static inhomogeneities and thermal fluctuations[7,8] taken into account by $I_{network}(q)$. Finally, $I_{PS}(q)$ denotes the scattering intensity which is caused by the density fluctuations of the solid PS core of the particles.[5,6] In the following these terms and their interrelation will be discussed.

For spherical symmetric particles with radius $R$ $I_{CS}(q)$ is equal to $B^2(q)$ where the scattering amplitude $B(q)$ is given by[9]

$$B(q) = 4\pi\int_0^R[\rho(r) - \rho_m]r^2\frac{\sin(qr)}{qr}\,dr \qquad (2)$$

* To whom all correspondence should be addressed. E-mail: Matthias.Ballauff@chemie.uni-karlsruhe.de.

10.1021/ma980985t CCC: $15.00 
Published on Web 11/19/1998

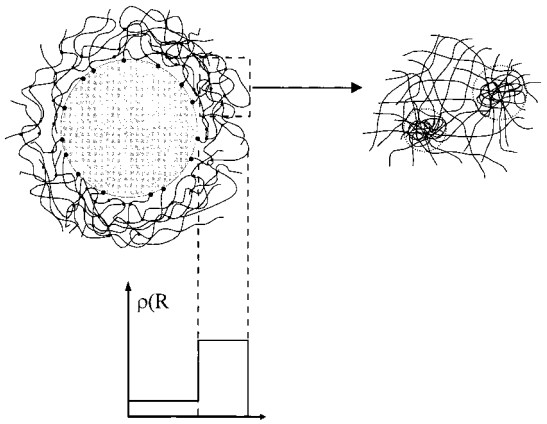


**Figure 1.** Analysis of core−shell microgels by SAXS according to eq 1: The term $I_{CS}(q)$ which is dominant at low $q$ values refers to a core−shell particle with the excess electron density $\rho(R)$. The network exhibits static and dynamic inhomogeneities which lead to $I_{network}(q)$. Finally, the polystyrene cores of the particles are not entirely homogeneous, but the density of the solid polystyrene fluctuates weakly around a mean value. This gives the third term $I_{PS}(q)$ which gives a small but nonnegligible contribution to $I(q)$. As discussed in the text, all three contributions to $I(q)$ derive from statistically independent fluctuations of the electron density in the system. Hence, the respective scattering intensities add up as stated by eq 1.

Here, $\rho(r) - \rho_m$ denotes the radial excess electron density which has been depicted in Figure 1 and $\rho_m$ is the electron density of the medium. In the course of the analysis to be conducted here it is important to realize that $I_{CS}(q)$ will decrease with $q^{-4}$ at sufficiently high $q$ (Porod's law[9]) if the core−shell particles have sharp interfaces. For particles with diffuse interfaces $I_{CS}(q)$ will diminish even more at high $q$.[10] Model calculations and previous experimental studies on core−shell particles[5,6] therefore suggest that $I_{CS}(q)$ of the present particles will decrease by 2−3 orders of magnitude in the range $0 < q < 0.2$ nm$^{-1}$.

Equation 2 can easily be generalized to include polydisperse systems of noninteracting systems. In this case the intensities $B_i^2(q)$ of the species $i$ are added up, weighted by their respective number density $N_i$. A discussion of this point and the consequences of a size distribution of finite width have been published recently.[5,6] Here, it suffices to mention that the polydispersity smears out the deep minima of $I_{CS}(q)$ to a certain extent.

The second term $I_{network}(q)$ is caused by the spatial inhomogeneities of the network in the shell. Following the theoretical analysis of Panyukov and Rabin,[7] the intensity $I_{network}(q)$ of macroscopic polymeric networks can be decomposed into two terms: (i) a contribution $C(q)$ derived from the static spatial inhomogeneity of the network and (ii) a contribution $G(q)$ due to the thermal density fluctuation of the network. Figure 1 gives a pictorial representation of these terms. Depending on the degree of cross-linking, the local density of the polymer segments will fluctuate in a manner similar to the concentration fluctuations in a concentrated polymer solution, giving rise to the term $G(q)$. In addition to this, the degree of cross-linking exhibits a spatial variation which had been affixed in the process of network formation. Hence, $C(q)$ derives from static variations of the local polymer density shown schematically in Figure 1.

The theory of Panyukov and Rabin[7] derives both contributions without additional assumptions by treating a system of instantaneously cross-linked Gaussian chains with excluded volume. The result depends explicitly on the polymer volume fraction in the gel at preparation and at measurement. This theory has met with gratifying success when compared to recent experimental data.[8] It is not clear, however, whether this theory can directly be applied to the restricted microscopic system under consideration here. In addition to this, no direct information is available on the volume fraction at preparation.

For the evaluation of the present data it therefore seems to be more appropriate to use an empirical decomposition of the $I_{network}(q)$ used in previous analyses of networks by SANS.[1,8,11−13] Hence,

$$I_{network}(q) = I_{in}(q) + I_{fluct}(q) = I_{in}(0)\exp[-R_g^2q^2] + \frac{I_{fluct}(0)}{1+\xi^2q^2} \quad (3)$$

where $I_{in}(q)$ and $I_{fluct}(q)$ refer to the static part of $I_{network}(q)$ and to the part caused by thermal fluctuations, respectively. In this context $I_{in}(0)$ and $I_{fluct}(0)$ are treated as adjustable parameters. The quantity $R_g$ denotes the radius of gyration of the static inhomogeneities (see Figure 1) whereas $\xi$ is the correlation length of the thermal fluctuations.

This analysis has been used successfully to explain the scattering from macroscopic PNIPA networks in a quantitative fashion.[13] In the course of this study the radius of gyration $R_g$ of PNIPA gels has been found to be of the order of 10−14 nm.[13] Furthermore, this parameter is virtually independent of temperature.[13] The correlation length of PNIPA macronetworks has been found to be of the order of a few nanometers if measured well-below the spinodal temperature $T_S$ of the network[13] whereas $\xi$ diverges when approaching $T_S$.

The third term of eq 1, $I_{PS}(q)$, is the small but nonnegligible contribution to $I(q)$ caused by the density fluctuations of the solid PS core. This term and its magnitude have been discussed at length recently in the course of the SAXS analysis of composite latex particles.[5,6]

The second and the third term in eq 1 refer to fluctuations of the scattering length density which are independent of each other. It is furthermore evident that $I_{fluct}(q)$ and $I_{PS}(q)$ derive from fluctuations which are not coupled to the radial core−shell structure of the particles. As a consequence of this independence, the intensities of the three contributions add up and not the amplitudes. Regarding $I_{in}(q)$, it may be assumed that the static inhomogeneities are distributed at random in the shell. In this case the fluctuations giving rise to $I_{in}(q)$ are fully decoupled from the profile $\rho(r) - \rho_m$. No cross-term appears between the three terms and eq 1 possesses complete generality. Only if the static inhomogeneities are mainly located at, for example, the periphery of the shell will they change the profile $\rho(r) - \rho_m$ and thus influence $I_{CS}(q)$ to a certain extent.

Given the additivity of the three terms according to eq 1 we now discuss the decomposition; it is evident that $I_{CS}(q)$ will dominate $I(q)$ at small $q$. This is due to the fact that $I_{CS}(q)$ refers to the entire core−shell particle, the diameter of which is between 120 and 160 nm. This also implies that $I_{CS}(q)$ will decrease most rapidly with increasing $q$ as discussed above. The term $I_{network}(q)$ refers to inhomogeneities and thermal fluctuations of the network. Previous SANS studies[13] demonstrated

that the characteristic length scale $R_g$ is of the order of 10 nm (cf. above) whereas $\xi$ governing $I_{fluct}(q)$ is expected to be of the order of a few nanometers far-below the transition. Since the contributions at $q = 0$ scale with $R_g^3$ or with $\xi^3$, respectively, they may be neglected at small $q$ to a good approximation. As a consequence of this, $I(q)$ measured up to $q \approx 0.2$ nm$^{-1}$ can be described solely by $I_{CS}(q)$ while all other terms may be dismissed in this $q$ range. However, $I_{CS}(q)$ will be greatly diminished for $q > 0.2$ nm$^{-1}$ and $I_{fluct}(q)$ will become the leading term at a higher scattering angle. The subtraction of $I_{PS}(q)$ provides no difficulty because this term can be determined from SAXS measurements of the core latex. By virtue of these propitious facts a decomposition of $I(q)$ into the three terms of eq 1 becomes possible.

## Experimental Section

**Materials.** *N*-Isopropylacrylamide (Polyscience, analytical grade), *N*,*N*′-methylenebisacrylamide (BIS; Fluka), and sodium dodecyl sulfate (SDS; Fluka) were used as received. The initiator potassium peroxodisulfate (KPS; Fluka) was recrystallized from deionized water. Styrene (BASF) was destabilized by washing with aqueous NaOH and subsequently with deionized water. After careful drying with $CaCl_2$ the monomer is distilled in vacuo. Water was purified using reverse osmosis (MilliRO; Millipore) and ion exchange (MilliQ; Millipore). The deionized $H_2O$ thus obtained had a conductivity less than 0.05 $\mu$S/cm. It was filtered through a 0.2 $\mu$m PTFE filter supplied by Millipore.

**Emulsion Polymerizations; Core Latex.** Emulsion polymerization has been done using a 1-L flask equipped with a stirrer, a reflux condenser, and a thermometer. The recipe for the core latex is given in the following: SDS (1.50 g) and NIPA (7.5 g) were dissolved in pure water (525 g) with stirring and the solution is degassed by repeated evacuation. After addition of styrene (142.5 g), the mixture is heated to 80 °C under an atmosphere of nitrogen. The initiator KPS (0.352 g dissolved in 15 mL of water) is added while the mixture is stirred with 400 rpm. After 8 h the latex is cooled to room temperature and filtered through glass wool to remove traces of coagulum. Purification was done by dialysis of the latex against $2.5 \times 10^{-3}$ M KCl solution for approximately 3 weeks.

**Core−Shell Latex.** The seeded emulsion polymerization for the core−shell system under consideration here was done using 100 g of the core latex diluted with 320 g of deionized water together with 20 g of NIPA and 1.43 g of BIS. No additional SDS was added in this step. After this stirred mixture has been heated to 80 °C, the reaction is started by the addition of 0.201 g of KPS (dissolved in 15 mL of water) and the entire mixture is allowed to stir for 4 h at this temperature. After cooling to room temperature the latex has been purified by exhaustive serum replacement against purified water (membrane: cellulose nitrate with a 0.05-$\mu$m pore width supplied by Schleicher & Schuell).

**Methods.** The weight fraction of the seed as well as the core−shell system was determined gravimetrically. The density of the latex particles was determined using a DMA-60 densitometer supplied by PAAR (Graz, Austria). The size of the particles and their size distribution were determined by the use of transmission electron microscopy (TEM, Hitachi 700).

Small-angle X-ray scattering (SAXS) was done either using a commercial Kratky camera ($0.08 \le q \le 5$ nm$^{-1}$) equipped with a one-dimensional counter (Braun, München)[5] or by using an improved Kratky camera ($0.03 \le q \le 4$ nm$^{-1}$) described elsewhere.[6,14] For both camera systems the evaluation of the scattering intensities included the following steps:[5,6,14] At first, the background scattering by the dispersion medium water and by the sample holder is subtracted and the scattering intensities are normalized to the intensity of the incident beam. Afterward, the desmearing for slit height and slit length is effected according to the procedures described in ref 14 and in refs 5 and 6. The concentration of the latexes during all measurements was 7 wt %.

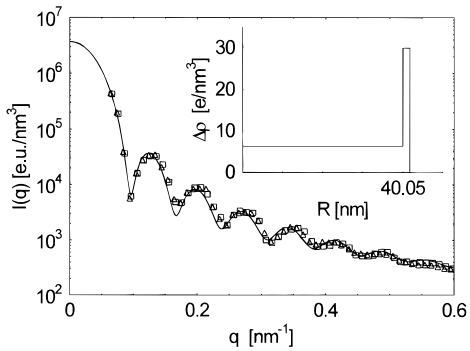


**Figure 2.** SAXS intensities $I(q)$ of the core particles below the volume transition (25 °C, squares) and above the volume transition (50 °C, triangles). The solid line display the fit of $I(q)$ by the radial excess electron density shown in the inset. The comparison of the SAXS data taken at both temperatures demonstrates the core to be independent of temperature.

In the course of the present SAXS analysis the influence of concentration is negligible. The structure factor $S(q)$ of a dilute system of spherical latex particles has been discussed at length recently,[5,6] leading to the following result: For the latex concentrations used here (ca. 7 wt %) the structure factor $S(q)$ differs from 1 only in a $q$ range smaller than the smallest $q$ accessible for the present SAXS cameras. For higher $q$ values $S(q) \approx 1$ within experimental uncertainty and the influence of interparticular interferences can be dismissed without problems.

## Results and Discussion

**Core Latex.** The core latex consisting of 95 wt % PS and 5 wt % PNIPA has been made by using the ionic initiator potassium peroxodisulfate. This leads to chemically bound sulfate groups on the surface of the core which helps to stabilize the particles above the volume transition where the steric stabilization by the polymer chains of the shell is not fully operative anymore (cf. below). Additional experiments using particles without chemically bound charges showed that flocculation sets in at temperatures above the volume transition.

Figure 2 displays the SAXS intensities of the core particles obtained at 25 °C (squares) and at 50 °C (triangles). Both scattering curves coincide with experimental uncertainty. This demonstrates clearly that the core is absolutely independent of temperature despite a small amount of added PNIPA chains. The SAXS analysis of the core particles given in Figure 2 demonstrates furthermore that the small fraction of PNIPA is located in a thin shell at the surface. This can be seen from the inset of Figure 2, showing the radial electron density of the core latex. As mentioned above, PNIPA has a much higher electron density as solid PS. The thin shell (1.8 nm) exhibiting a considerably higher electron density of 30 e$^-$/nm$^3$ (as compared to 45.8 e$^-$/nm$^3$ for PNIPA; see below) demonstrates that the PNIPA chains have been enriched at the surface of the core particles. The fit procedure also shows that the size distribution of the core particles is rather small (standard deviation: 5.8%).

The SAXS data taken from the core particles furthermore serves for the determination of $I_{PS}(q)$ (i.e., the contribution to the SAXS intensity due to the density fluctuations of the solid PS). As in previous cases this contribution may be described by $I_{PS}(q) = a \exp(bq^2)$ (cf. the discussion of this point in ref 5). Fits of this expression to the SAXS data between $q = 2$ and 4 nm$^{-1}$ treating $a$ and $b$ as adjustable parameters then leads to the determination of $I_{PS}(q)$ which may be removed from I(q) of the core−shell system (see eq 1).

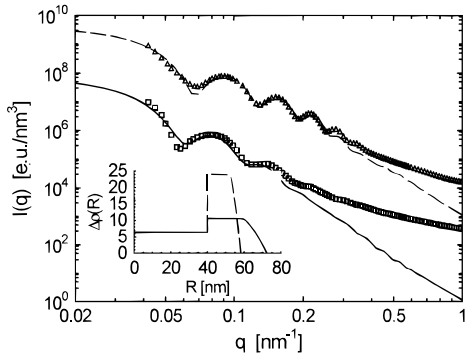


**Figure 3.** Measured SAXS intensities $I(q)$ of the core−shell particles below the volume transition (25 °C, squares) and above the volume transition (50 °C, triangles). For the sake of clarity the data measured at 50 °C have been multiplied by 100. The lines display the fit of $I_{CS}(q)$ (cf. eq 1) to the data at low $q$ values ($q < 0.2$ nm$^{-1}$; 25 °C, solid line; 50 °C, dashed line). The radial excess electron density $\Delta\rho(R)$ derived from this fit is shown in the inset. The marked deviation between $I(q)$ and $I_{CS}(q)$ seen at high $q$ values is due to the thermal fluctuations of the network in the shell.

**Core−Shell Particles.** The pure PNIPA shell is generated on the surface of these particles in a second emulsion polymerization using *N*-isopropylacrylamide (NIPA) as a monomer and *N*,*N*′-methylenebisacrylamide (BIS) as a cross-linker (molar ratio of NIPA to BIS: 95/5). The temperature of this polymerization (80 °C) is far above that of the volume transition of PNIPA gels (34 °C; ref 1). The network constituting the shell is thus formed under poor solvent conditions. Latex stabilization in this stage is solely achieved by the surface charges stemming from the initiator KPS, which was used for the synthesis of the cores.

Transmission electron microscopy (TEM) demonstrated that the strictly spherical particles exhibit a narrow size distribution with a standard deviation below 7%. This shows that the core−shell latex presents a well-defined system which is amenable for a comprehensive analysis by SAXS.

The SAXS intensity of the core−shell latex have been measured at two temperatures: At 25 °C where water is a good solvent for PNIPA and far above the transition temperature at 50 °C. Additional measurements by dynamic light scattering (DLS) indicated that the volume transition in the PNIPA shell is continuous.[15] This is also expected from experiments done with PNIPA macrogels which had been prepared with a similar ratio of NIPA to BIS as employed herein.[16,17] Hence, precise measurements done at two characteristic states of the microgel suffice to elucidate the salient features of the volume transition in the core−shell particles.

Figure 3 displays $I(q)$ obtained at 25 °C (squares) and at 50 °C (triangles). For the sake of clarity the latter curve has been multiplied by 100. The SAXS intensity taken at 50 °C demonstrates that no aggregation or coagulation has taken place because of the electrostatic stabilization discussed above.

The above discussion has shown that $I_{CS}(q)$ and $I_{network}(q)$ contribute in different $q$ ranges because the latter contribution decreases with $q^{-2}$ at high $q$ (see eq 3) whereas $I_{CS}(q)$ decreases with $q^{-4}$. Thus, the decomposition of $I(q)$ may be done as follows: First, $I_{PS}(q)$ obtained from the core latex (see above) is subtracted from the measured intensity $I(q)$. $I_{PS}(q)$ is only a minor contribution to $I(q)$ (maximal contribution: 5% of $I(q)$ at $q = 1$ nm$^{-1}$) but must be subtracted properly from $I(q)$ when analyzing the remaining parts $I_{CS}(q)$ and $I_{network}(q)$.

In a second step $I_{CS}(q)$ is determined from $I(q)$, taking into account only the data in the $q$ range smaller than 0.2 nm$^{-1}$. The lines in Figure 3 show the respective fits achieved by the fit routine described recently.[14] For this fit the polydispersity and the size of the core particles has directly been taken from the above SAXS analysis of the seed latex. Only the polydispersity of the shell thickness has been treated as an adjustable parameter. The resulting standard deviation (12.3% at 25 °C; 7.8% at 50 °C) is greater than the respective value for the core particles.

The excess electron densities $\rho(R) - \rho_m$ resulting from this fit are displayed in the inset of Figure 3 where $\rho_m$ is the electron density of water. The profiles $\Delta\rho(R) = \rho(R) - \rho_m$ shown in the inset of Figure 3 indicate the swelling of the PNIPA shell when going from poor solvent conditions (50 °C; dashed lines) to good solvent conditions (25 °C; solid lines). Admittedly, the $q$ range used for the present fits is rather small. The discussion in refs 5,6 demonstrates, however, that the zeroth and second moment of the profile may be derived from this fit in a secure manner. Its exact shape cannot be determined from the present data.

The zeroth moment of the distribution $\rho(R) - \rho_m$ (i.e., the entire number of excess electrons) may also serve for additional proof of consistency because this quantity may be estimated in good approximation from the mass of the PNIPA chains in the shell and the partial specific volume of PNIPA in water (0.877 cm$^3$/g; ref 13). The excess electron density of the PNIPA chains in water follows from this as 45.8 e$^-$/nm$^3$ which exceeds largely the respective value of the polystyrene core (6.4 e$^-$/nm$^3$; cf. ref 5). Since virtually all NIPA used in the synthesis has been built into the shell, the zeroth moment of $\rho(R) - \rho_m$ may serve as a sensitive check of the fit of $I_{CS}(q)$. Here, the data derived from the fit and the data obtained from mass balance agreed within a few percentage points.

No profile $\rho(R) - \rho_m$ can modify $I_{CS}(q)$ so that the fit describes the data at higher $q$ values as well. As discussed above, this is a consequence that $I_{CS}(q)$ must scale at least with $q^{-x}$ at higher $q$ where $x \geq 4$.[9] The strong intensity observed at both temperatures for $q > 0.3$ nm$^{-1}$ must therefore be traced back to the contribution $I_{network}(q)$.

From the profile shown in the inset in Figure 3 the average volume fraction $\phi$ of PNIPA can be estimated to be 0.5 at 50 °C whereas a value of 0.23 follows from the SAXS analysis at 25 °C. At a low temperature the shell has an extension of approximately 32 nm which shrinks to 18 nm above the transition. This corresponds to a shrinking of the volume of the shell by a factor of 2.2 which is small compared to PNIPA macrogels having a similar degree of cross-linking.[16,17] In addition to this, the gel does not collapse but remains swollen to a certain extent even far-above the volume transition.

Having shown that $I_{CS}(q)$ may be obtained from $I(q)$ taken at low $q$, the remaining terms given in eq 1 may now be analyzed as follows: The contribution $I_{CS}(q)$ derived from the above fit is subtracted from $I(q)$. Having already subtracted $I_{PS}(q)$, we thus obtain the contribution of the network $I_{network}(q)$. As discussed in the theoretical section, the functional form of $I_{network}(q)$ at high $q$ may be approximated by eq 3.

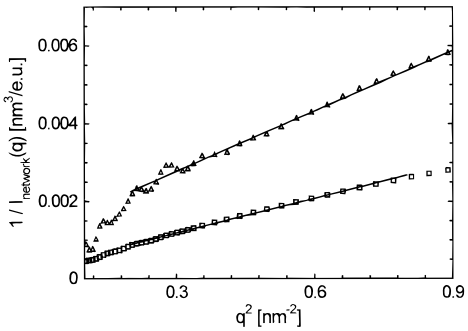


**Figure 4.** Analysis of $I_{network}(q) = I(q) - I_{CS}(q) - I_{PS}(q)$ as determined from the decomposition of $I(q)$ according to eq 1: Plot of $I_{network}(q)^{-1}$ vs $q^2$ (cf. eq 3) in the $q$ range where the measured scattering intensity $I(q)$ is governed by the contribution of the network in the shell. The correlation length $\xi$ derived from these fits is $\xi = 3.2$ nm below the volume transition (squares, 25 °C) and $\xi = 2.1$ nm above the volume transition (triangles, 50 °C).

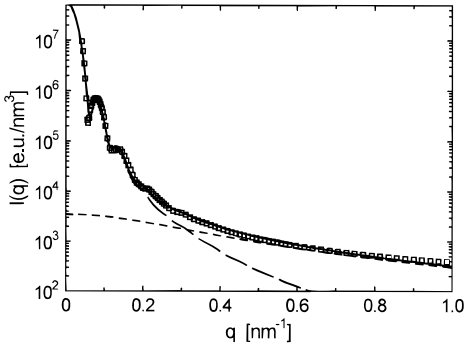


**Figure 5.** Comparison of $I_{CS}(q)$ (long-dashed line) and $I_{fluct}(q)$ (short-dashed line) with the scattering intensity $I(q) - I_{PS}(q)$ measured at 25 °C (squares). The solid line gives $I_{CS}(q) + I_{fluct}(q)$ (cf. eq 3). See text for further explanations.

Figure 4 displays a plot of the reciprocal of $I_{network}(q)$ against $q^2$. Good linearity is seen for $q > 0.5$ nm$^{-1}$ for both temperatures. Only at lower $q$ deviations are seen. It must be kept in mind, however, that the respective $q$ ranges in which the three terms in eq 1 are prominent are not separated in a strict manner. Moreover, $I_{in}(q)$ is expected to contribute at lower $q$ than $I_{fluct}(q)$ (cf. Theory section). The linearity seen in Figure 4 suggests that of the two terms defined in eq 3 only $I_{fluct}(q)$ contributes appreciably in the $q$ range accessible to the present analysis. $I(q)$ appears to be mainly governed by the thermal fluctuations of the network. The analysis of the data shown in Figure 3 leads to $\xi = 3.2$ nm at 25 °C whereas $\xi = 2.1$ nm at 50 °C. This is slightly smaller than the values of $\xi$ which have been found in the case of PNIPA macrogels at the same temperature recently.[13]

We therefore conclude from this analysis that $I_{CS}(q)$ together with $I_{fluct}(q)$ are the leading terms in eq 1 and may be obtained by the above analysis. This can also be seen directly from a comparison of the measured scattering intensity $I(q)$ with these two main contributions displayed in Figure 5. Here, the addition of the $I_{CS}(q)$ and $I_{fluct}(q)$ describe the scattering intensity $I(q) - I_{PS}(q)$ in very good approximation which lends support to the present way of analyzing the SAXS data.

From these findings it becomes obvious that the cross-linked spherical brushes under consideration here behave differently than macrogels.[16,17] The change of volume during the transition also is smaller than the one observed for submicron gel beads consisting entirely of cross-linked PNIPA chains. Data presented by Hirose et al.[18] show that PNIPA microbeads exhibit a swelling ratio of more than 10. Although the degree of cross-linking has been slightly smaller than that in the case of core−shell micronetworks studied here, it seems to be safe to conclude that the volume transition in the case of PNIPA microbeads leads to greater swelling ratios. Aside from a quantitative comparison of the respective parameters, the present analysis has also demonstrated that the network in the shell remains in a fluidlike state characterized by local density fluctuations even above the volume transition. This is in accord with a rather small swelling ratio derived from the analysis of $I_{CS}(q)$ (see inset of Figure 3).

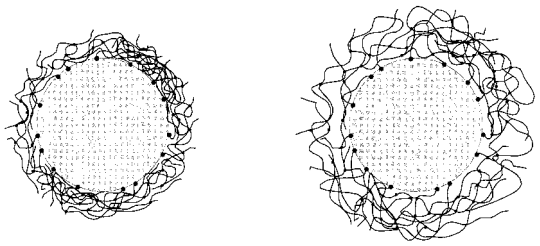


**Figure 6.** Schematic representation of the volume transition in core−shell micronetworks: The polymer chains are affixed to the surface of the core which thus provides one boundary of the network. Swelling can only take place by moving the outer boundary. The analysis of the SAXS data shows that the volume transition in this system is less pronounced than that in macrogels which can be traced back to the spatial constraint exerted by the core−shell morphology of the network.

The reason for this difference is easily explained by the geometrical constraint to which the present gel is subjected. Most of the PNIPA chains are affixed to a solid spherical surface as depicted in Figure 6. Therefore, the chains can only shrink along the direction of the surface normal; no marked contraction can result parallel to the surface. Hence, if the unconstrained gel shrinks by a factor of 10, the corresponding shrinking of the microgel layer is expected to be of the order $(10)^{1/3} \approx 2.15$ which is of the order observed in the present system. This type of spatial constraint may be compared to external uniaxial forces (cf. the discussion of this point by Khokhlov et al.[19]). It is obvious that the restricted shrinking leads to a network in which thermal fluctuation may persist even above the volume transition. This is in accord with the finding that $I_{fluct}(q)$ represents an important contribution to $I(q)$ even at 50 °C (cf. the discussion of Figures 3 and 4).

Core−shell micronetworks therefore present an interesting class of gels in which the chains are subjected to geometric constraints. It is therefore interesting to see whether charges in the network may lead to a discontinuous transition as those observed in the corresponding macrogels (cf. the discussion of this point by Shibayama[8]). Work in this direction is underway.

**Acknowledgment.** Financial support by the Bundesministerium für Forschung und Technologie and by the Deutsche Forschungsgemeinschaft is gratefully acknowledged.

## References and Notes

(1) Shibayama, M.; Tanaka, T. *Adv. Polym. Sci.* **1993**, *109*, 1; cf. also further reviews in this volume and volume 110.

(2) Makino, K.; Yamamoto, S. Fujimoto, K.; Kawaguchi, H.; Oshima, H. *J. Colloid Interface Sci.* **1994**, *166*, 251.
(3) Okubo, M.; Ahmad, H. *Colloid Polym. Sci.* **1996**, *274*, 112.
(4) Dong, L.; Hoffman, A. S. *J. Controlled Release* **1991**, *15*, 141.
(5) Ballauff, M.; Bolze, J.; Dingenouts, N.; Hickl, P.; Pötschke, D. *Macromol. Chem. Phys.* **1996**, *197*, 3043.
(6) Dingenouts, N.; Bolze, J.; Pötschke, D.; Ballauff, M. *Adv. Polym. Sci.* **1998**, accepted for publication.
(7) Panyukov, S.; Rabin, Y. *Macromolecule*s **1996**, *29*, 7960; Panyukov, S.; Rabin, Y. *Phys. Rep.* **1995**, *269*, 1.
(8) Shibayama, M. *Macromol. Chem. Phys.* **1998**, *199*, 1.
(9) Glatter, O., Kratky, O., Eds. *Small Angle X-ray Scattering*; Academic Press: London, 1982.
(10) Siemann, U.; Ruland, W. *Colloid Polym. Sci.* **1982**, *260*, 999.
(11) Horkay, F.; Hecht, A.-M.; Mallam, S.; Geissler, E.; Rennie, A. R. *Macromolecules* **1991**, *24*, 2896.
(12) Geissler, E.; Horkay, F.; Hecht, A.-M. *Phys. Rev. Lett.* **1993**, *71*, 645.
(13) Shibayama, M.; Tanaka, T.; Han, C. *J. Chem. Phys.* **1992**, *97*, 6829.
(14) Dingenouts, N.; Ballauff, M. *Acta Polym.* **1998**, *49*, 178.
(15) Norhausen, C.; Dingenouts, N.; Ballauff, M. in preparation.
(16) Hirotsu, S. *Adv. Polym. Sci.* **1993**, *110*, 1.
(17) Li, Y.; Tanaka, T. *J. Chem. Phys.* **1989**, *90*, 5161.
(18) Hirose, Y.; Amiya, T.; Hirokawa, Y.; Tanaka, T. *Macromolecules* **1987**, *20*, 1342.
(19) Khokhlov, A.; Starodubtzev, S. G.; Vasilevskaya, V. V. *Adv. Polym. Sci.* **1993**, *109*, 123.

MA980985T